Journal of Process Control 21 (2011) 1296–1305

Contents lists available at ScienceDirect

Journal of Process Control

journal homepage: www.elsevier.com/locate/jprocont

Model predictive control of nonlinear singularly perturbed systems: Application to a large-scale process network

Xianzhong Chen[a], Mohsen Heidarinejad[b], Jinfeng Liu[a], David Muñoz de la Peña[c], Panagiotis D. Christofides[a,b,*]

[a] Department of Chemical and Biomolecular Engineering, University of California, Los Angeles, CA 90095-1592, USA
[b] Department of Electrical Engineering, University of California, Los Angeles, CA 90095-1592, USA
[c] Departamento de Ingeniería de Sistemas y Automática, Universidad de Sevilla, Sevilla 41092, Spain

ARTICLE INFO

Article history:
Received 17 March 2011
Received in revised form 11 July 2011
Accepted 12 July 2011
Available online 17 August 2011

Keywords:
Two-time-scale processes
Model predictive control
Distributed predictive control
Nonlinear processes

ABSTRACT

This work focuses on model predictive control of nonlinear singularly perturbed systems. A composite control system using multirate sampling (i.e., fast sampling of the fast state variables and slow sampling of the slow state variables) and consisting of a "fast" feedback controller that stabilizes the fast dynamics and a model predictive controller that stabilizes the slow dynamics and enforces desired performance objectives in the slow subsystem is designed. Using stability results for nonlinear singularly perturbed systems, the closed-loop system is analyzed and sufficient conditions for stability are derived. A large-scale nonlinear reactor-separator process network which exhibits two-time-scale behavior is used to demonstrate the controller design including a distributed implementation of the predictive controller.

1. Introduction

Chemical processes and plants are characterized by nonlinear behavior and strong coupling of physico-chemical phenomena occurring at disparate time-scales. Examples include fluidized catalytic crackers, distillation columns, biochemical reactors as well as chemical process networks in which the individual processes evolve in a fast time-scale and the network dynamics evolve in a slow time-scale. Singular perturbation theory provides a natural framework for modeling, analysis, order reduction and controller design for nonlinear two-time-scale processes (e.g., [1,2]). Within this framework, methods for controller design based on optimal control (e.g., [3]), geometric control (e.g., [1,2]) and Lyapunov-based control [4] have been developed.

Model predictive control (MPC) is a practically important control framework which can be used to design and coordinate control systems and can explicitly handle input and state constraints. MPC utilizes a model to predict the future evolution of the plant at each sampling time according to the current state over a given prediction horizon. MPC utilizes these predictions in an on-line optimization framework to obtain an optimal control input trajectory which minimizes an objective function subject to state and input constraints. To reduce the dimensionality and computational burden of the optimization problem, optimization is performed over the set of piecewise constant trajectories with fixed sampling time and finite prediction horizon. Once the optimization problem is solved, only the first step of the optimal input is implemented by the actuators, the rest of the trajectory is discarded and the optimization is repeated in the next sampling step (e.g., [5,6]). In [7], a Lyapunov-based MPC (LMPC) design was proposed by incorporating a Lyapunov function based constraint in the MPC optimization problem to guarantee the closed-loop stability. This LMPC design inherits the stability properties of a pre-existing Lyapunov-based controller and has an explicitly characterized stability region. In the context of control of large-scale process networks within a centralized MPC framework, the computational complexity of MPC may increase significantly with the increase of the number of state variables and manipulated inputs. Moreover, a centralized control system for large-scale systems may be difficult to organize and maintain and is vulnerable to potential process faults. To overcome these issues, distributed MPC (DMPC) can be utilized. In a DMPC framework, optimal input trajectories are obtained by solving a number of lower-dimension MPC problems compared to the fully centralized MPC (see, e.g., [8–10]). In the context of MPC of singularly perturbed systems, most of the efforts have been dedicated to linear systems [11] or to MPC of specific classes of two-time-scale processes [12,13].

* Corresponding author at: Department of Chemical and Biomolecular Engineering, 5531 Boelter Hall, University of California, Los Angeles, CA 90095-1592, USA. Tel.: +1 310 7941015; fax: +1 310 206 4107.
E-mail address: pdc@seas.ucla.edu (P.D. Christofides).

0959-1524/$ – see front matter © 2011 Elsevier Ltd. All rights reserved.
doi:10.1016/j.jprocont.2011.07.004

This work focuses on model predictive control of nonlinear singularly perturbed systems in standard form where the separation between the fast and slow state variables is explicit. A composite control system using multirate sampling (i.e., fast sampling of the fast state variables and slow sampling of the slow state variables) and consisting of a "fast" feedback controller that stabilizes the fast dynamics and a model predictive controller that stabilizes the slow dynamics and enforces desired performance objectives in the slow subsystem is designed. Using stability results for nonlinear singularly perturbed systems, the closed-loop system is analyzed and sufficient conditions for stability are derived. A large-scale nonlinear reactor-separator process network is used to demonstrate the application of the method including a distributed implementation of the predictive controller.

2. Preliminaries

2.1. Notation

The operator $|\cdot|$ is used to denote Euclidean norm of a vector and the symbol Ω_r is used to denote the set $\Omega_r := \{x \in R^{n_x} : V(x) \leq r\}$ where V is a positive definite scalar function. For any measurable (with respect to the Lebesgue measure) function $w : R_{\geq 0} \to R^l$, $||w||$ denotes ess.sup.$|w(t)|$, $t \geq 0$. A function $\gamma : R_{\geq 0} \to R_{\geq 0}$ is said to be of class K if it is continuous, nondecreasing, and is zero at zero. A function $\beta : R_{\geq 0} \times R_{\geq 0} \to R_{\geq 0}$ is said to be of class KL if, for each fixed t, the function $\beta(\cdot, t)$ is of class K and, for each fixed s, the function $\beta(s, \cdot)$ is nonincreasing and tends to zero at infinity.

2.2. Class of nonlinear singularly perturbed systems

In this work, we focus on nonlinear singularly perturbed systems in standard form with the following state-space description:

$$\begin{aligned} \dot{x} &= f(x, z, \epsilon, u_s, w), \quad x(0) = x_0 \\ \epsilon \dot{z} &= g(x, z, \epsilon, u_f, w), \quad z(0) = z_0 \end{aligned} \tag{1}$$

where $x \in R^n$ and $z \in R^m$ denote the vector of state variables, ϵ is a small positive parameter, $w \in R^l$ denotes the vector of disturbances and $u_s \in U \subset R^p$ and $u_f \in V \subset R^q$ are two sets of manipulated inputs. The sets U and V are nonempty convex sets which are defined as follows:

$$\begin{aligned} U &:= \{u_{s,i}(t) : |u_{s,i}(t)| \leq u_{s,i}^{\max}, i \in [1, p]\} \\ V &:= \{u_{f,j}(t) : |u_{f,j}(t)| \leq u_{f,j}^{\max}, j \in [1, q]\} \end{aligned} \tag{2}$$

where $u_{s,i}^{\max}$ and $u_{f,j}^{\max}$ are positive real numbers, specifying the input constraints. The disturbance vector is assumed to be absolutely continuous and bounded, i.e., $W := \{w(t) \in R^l : |w(t)| \leq \theta\}$ where θ is a positive real number. Since the small parameter ϵ multiplies the time derivative of the vector z in the system of Eq. (1), the separation of the slow and fast variables in Eq. (1) is explicit, and thus, we will refer to the vector x as the slow states and to the vector z as the fast states. We assume that the vector fields f and g are locally Lipschitz in $R^n \times R^m \times [0, \bar{\epsilon}) \times R^p \times R^q \times R^l$ for some $\bar{\epsilon} > 0$ and that the origin is an equilibrium point of the unforced nominal system (i.e., system of Eq. (1) with $u_s = 0$, $u_f = 0$ and $w = 0$).

With respect to the control problem formulation, we assume that the fast states z are sampled continuously and their measurements are available for all time t (e.g., variables for which fast sampling is possible usually include temperature, pressure and hold-ups) while the slow states x are sampled synchronously and are available at time instants indicated by the time sequence $\{t_{k \geq 0}\}$ with $t_k = t_0 + k\Delta$, $k = 0, 1, \ldots$ where t_0 is the initial time and Δ is the sampling time (e.g., slowly sampled variables usually involve species concentrations). The set of manipulated inputs u_f is responsible for stabilizing the fast dynamics of Eq. (1) and for this set the control action is assumed to be computed continuously, while the set of manipulated inputs u_s is evaluated at each sampling time t_k and is responsible for stabilizing the slow dynamics and enforcing a desired level of optimal closed-loop performance.

2.3. Two-time-scale system decomposition

The explicit separation of the slow and fast variables in the system of Eq. (1) allows decomposing it into two separate reduced-order systems evolving in different time-scales. To proceed with such a two-time-scale decomposition and in order to simplify the notation of the subsequent development, we will first address the issue of stability of the fast dynamics. Since there is no assumption that the fast dynamics of Eq. (1) are asymptotically stable, we assume the existence of a "fast" feedback control law $u_f = p(x, z)$ that renders the fast dynamics asymptotically stable in a sense to be made precise in Assumption 2 below. Substituting $u_f = p(x, z)$ in Eq. (1) and setting $\epsilon = 0$ in the resulting system, we obtain:

$$\frac{dx}{dt} = f(x, z, 0, u_s, w) \tag{3a}$$

$$0 = g(x, z, 0, p(x, z), w) \tag{3b}$$

Assumption 1. The equation $g(x, z, 0, p(x, z), w) = 0$ possesses a unique root

$$z = \hat{g}(x, w) \tag{4}$$

with the properties that $\hat{g} : R^n \times R^l \to R^m$ and its partial derivatives $(\partial \hat{g}/\partial x)$, $(\partial \hat{g}/\partial w)$ are locally Lipschitz.

Assumption 1 is a standard requirement in singularly perturbation theory (see e.g., [3]) and it is made to ensure that the system has an isolated equilibrium manifold for the fast dynamics. On this manifold, z can be expressed in terms of x and w using an algebraic expression. This assumption does not pose any practical limitation in the process example below but it is a necessary one in the singular perturbation framework to construct a well-defined slow subsystem.

Using $z = \hat{g}(x, w)$, we can re-write Eq. (3) as follows:

$$\frac{dx}{dt} = f(x, \hat{g}(x, w), 0, u_s, w) =: f_s(x, u_s, w) \tag{5}$$

We will refer to the subsystem of Eq. (5) as the slow subsystem.

Introducing the fast time scale $\tau = (t/\epsilon)$ and the deviation variable $y = z - \hat{g}(x, w)$, we can rewrite the nonlinear singularly perturbed system of Eq. (1) as follows:

$$\begin{aligned} \frac{dx}{d\tau} &= \epsilon f(x, y + \hat{g}(x, w), \epsilon, u_s, w) \\ \frac{dy}{d\tau} &= g(x, y + \hat{g}(x, w), \epsilon, u_f, w) - \epsilon \frac{\partial \hat{g}}{\partial w} \dot{w} \\ &\quad - \epsilon \frac{\partial \hat{g}}{\partial x} f(x, y + \hat{g}(x, w), \epsilon, u_s, w) \end{aligned} \tag{6}$$

Setting $\epsilon = 0$, we obtain the following fast subsystem:

$$\frac{dy}{d\tau} = g(x, y + \hat{g}(x, w), 0, u_f, w) \tag{7}$$

where x and w can be considered as "frozen" to their initial values. Below we state our assumption on the stabilization of the fast subsystem:

Assumption 2. There exists a feedback control law $u_f = p(x, z) = p(x, y + \hat{g}(x, w)) \in V$ where $p(x, z)$ is a locally Lipschitz vector function of its arguments, such that the origin of the closed-loop fast subsystem:

$$\frac{dy}{d\tau} = g(x, y + \hat{g}(x, w), 0, p(x, y + \hat{g}(x, w)), w) \tag{8}$$

is globally asymptotically stable, uniformly in $x \in R^n$ and $w \in R^l$, in the sense that there exists a class KL function β_y such that for any $y(0) \in R^m$:

$$|y(t)| \leq \beta_y \left(|y(0)|, \frac{t}{\epsilon} \right) \tag{9}$$

for $t \geq 0$.

2.4. Lyapunov-based controller

We assume that there exists a Lyapunov-based locally Lipschitz control law $h(x) = [h_1(x) \ldots h_p(x)]^T$ with $u_{s,i} = h_i(x)$, $i = 1, \ldots, p$, which renders the origin of the nominal closed-loop slow subsystem asymptotically stable while satisfying the input constraints for all the states x inside a given stability region. The construction of such explicit stabilizing control laws can be readily done using Lyapunov techniques for specific classes of nonlinear systems, particularly input-affine nonlinear systems; the reader may refer to [16] for results and references in this area. Using converse Lyapunov theorems [14–16], this assumption implies that there exist functions $\alpha_i(\cdot)$, $i = 1, 2, 3, 4$ of class K and a continuously differentiable Lyapunov function $V(x)$ for the nominal closed-loop slow subsystem that satisfy the following inequalities:

$$\begin{aligned} &\alpha_1(|x|) \leq V(x) \leq \alpha_2(|x|) \\ &\frac{\partial V(x)}{\partial x} f_s(x, h(x), 0)) \leq -\alpha_3(|x|) \\ &h(x) \in U \end{aligned} \tag{10}$$

for all $x \in D \subseteq R^n$ where D is an open neighborhood of the origin. We denote the region $\Omega_\rho \subseteq D$ as the stability region of the closed-loop slow subsystem under the Lyapunov-based controller $h(x)$; Ω_ρ is typically taken to be a level set of $V(x)$. By continuity, the local Lipschitz property assumed for the vector fields $f_s(x, u_s, w)$ and taking into account that the manipulated inputs u_i, $i = 1, \ldots, p$, and the disturbance w are bounded in convex sets, there exists a positive constant M such that

$$|f_s(x, u_s, w)| \leq M \tag{11}$$

for all $x \in \Omega_\rho$, $u_s \in U$, and $w \in W$. In addition, by the continuous differentiable property of the Lyapunov function $V(x)$ and the Lipschitz property assumed for the vector field $f_s(x, u_s, w)$, there exist positive constants L_x and L_w such that

$$\begin{aligned} &\left| \frac{\partial V}{\partial x} f_s(x, u_s, w) - \frac{\partial V}{\partial x} f_s(x', u_s, w) \right| \leq L_x |x - x'| \\ &\left| \frac{\partial V}{\partial x} f_s(x, u_s, w) - \frac{\partial V}{\partial x} f_s(x, u_s, w') \right| \leq L_w |w - w'| \end{aligned} \tag{12}$$

for all $x, x' \in \Omega_\rho$, $u_s \in U$, and $w, w' \in W$.

2.5. Lyapunov-based MPC formulation

The longer sampling time of the slow state variables allows utilizing MPC to compute the control action u_s. A schematic of the proposed control system structure is shown in Fig. 1. Specifically, we use the LMPC proposed in [7] which guarantees practical stability of the closed-loop system and allows for an explicit characterization of the stability region to compute u_s. The LMPC is based on the Lyapunov-based controller $h(x)$. The controller $h(x)$ is used to define a stability constraint for the LMPC controller which guarantees that the LMPC controller inherits the stability and robustness properties of the Lyapunov-based controller $h(x)$. The LMPC controller is based on the following optimization problem:

$$\min_{u_s \in S(\Delta)} \int_0^{N_c \Delta} [\tilde{x}^T(\tau) Q_c \tilde{x}(\tau) + u_s^T(\tau) R_c u_s(\tau)] d\tau \tag{13a}$$

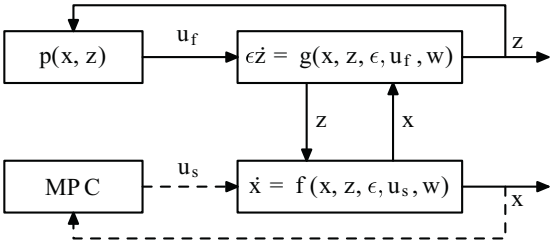

Fig. 1. A schematic of the proposed control system structure.

$$\text{s.t.}\, \dot{\tilde{x}}(\tau) = f_s(\tilde{x}(\tau), u_s, 0) \tag{13b}$$

$$u_s(\tau) \in U_s \tag{13c}$$

$$\tilde{x}(0) = x(t_k) \tag{13d}$$

$$\frac{\partial V(x(t_k))}{\partial x} f_s(x(t_k), u_s(0), 0) \leq \frac{\partial V(x(t_k))}{\partial x} f_s(x(t_k), h(x(t_k)), 0) \tag{13e}$$

where $S(\Delta)$ is the family of piece-wise constant functions with sampling period Δ, N_c is the prediction horizon, Q_c and R_c are positive definite weight matrices that define the cost, $x(t_k)$ is the state measurement obtained at t_k, $\tilde{x}$ is the predicted trajectory of the nominal system with u_s, the input trajectory computed by the LMPC of Eq. (13). The optimal solution to this optimization problem is denoted by $u_s^*(\tau | t_k)$, and is defined for $\tau \in [0, N_c \Delta)$.

The optimization problem of Eq. (13) does not depend on the uncertainty and guarantees that the system in closed-loop with the LMPC controller of Eq. (13) maintains the stability properties of the Lyapunov-based controller. The constraint of Eq. (13e) guarantees that the value of the time derivative of the Lyapunov function at the initial evaluation time of the LMPC is lower or equal to the value obtained if only the Lyapunov-based controller $h(x)$ is implemented in the closed-loop system in a sample-and-hold fashion. This is the constraint that allows proving that the LMPC inherits the stability and robustness properties of the Lyapunov-based controller. The manipulated inputs of the closed-loop slow subsystem under the LMPC controller are defined as follows

$$u_s(t) = u_s^*(t - t_k | t_k), \quad \forall t \in [t_k, t_{k+1}) \tag{14}$$

The main property of the LMPC controller is that the origin of the closed-loop system is practically stable for all initial states inside the stability region Ω_ρ for a sufficient small sampling time Δ and disturbance upper bound θ. The main advantage of LMPC approaches with respect to the Lyapunov-based controller is that optimality considerations can be taken explicitly into account (as well as constraints on the inputs and the states [7]) in the computation of the controller within an online optimization framework improving closed-loop performance.

Proposition 1 (cf. [7,17]). *Consider the slow subsystem of* Eq. (5) *in closed-loop under the LMPC design of* Eq. (14) *based on a Lyapunov-based controller $h(x)$ that satisfies the conditions of* Eq. (10). *Let $\epsilon_w > 0$, $\Delta > 0$ and $\rho > \rho_s > 0$, $\theta > 0$ satisfy the following constraint*:

$$-\alpha_3(\alpha_2^{-1}(\rho_s)) + L_x M \Delta + L_w \theta \leq -\frac{\epsilon_w}{\Delta} \tag{15}$$

There exists a class KL function β_x and a class K function γ such that if $x(0) \in \Omega_\rho$, then $x(t) \in \Omega_\rho$ for all $t \geq 0$ and

$$|x(t)| \leq \beta_x(|x(0)|, t) + \gamma(\rho^*) \tag{16}$$

with $\rho^* = \max \{V(x(t + \Delta)) : V(x(t)) \leq \rho_s\}$.

3. Stability analysis

The closed-loop stability of the system of Eq. (1) under the control of the controller $p(x, z)$ and the LMPC of Eq. (13) is established in the following theorem under appropriate conditions.

Theorem 1. *Consider the system of* Eq. (1) *in closed-loop with* $u_f = p(x, z)$ *and* u_s *determined by the LMPC of* Eq. (13) *based on a controller* $h(\cdot)$ *that satisfies the conditions of* Eq. (10). *Let also assumptions 1 and 2 and the condition of* Eq. (15) *hold. Then there exist functions* β_x *and* β_y *of class KL, a pair of positive real numbers* (δ, d) *and* $\epsilon^* > 0$ *such that if* $\max\{|x(0)|, |y(0)|, ||w||, ||\dot{w}||\} \leq \delta$ *and* $\epsilon \in (0, \epsilon^*]$, *then,*

$$\begin{aligned} |x(t)| &\leq \beta_x(|x(0)|, t) + \gamma(\rho^*) + d \\ |y(t)| &\leq \beta_y\left(|y(0)|, \frac{t}{\epsilon}\right) + d \end{aligned} \tag{17}$$

for all $t \geq 0$.

Proof. When $u_f = p(x, z)$ and $u_s = u_s^*$ is determined by the LMPC of Eq. (13), the closed-loop system takes the following form:

$$\begin{aligned} \dot{x} &= f(x, z, \epsilon, u_s^*, w), x(0) = x_0 \\ \epsilon\dot{z} &= g(x, z, \epsilon, p(x, z), w), z(0) = z_0 \end{aligned} \tag{18}$$

We will first compute the slow and fast closed-loop subsystems. Setting $\epsilon = 0$ in Eq. (18), we obtain:

$$\begin{aligned} \frac{dx}{dt} &= f(x, z, 0, u_s^*, w) \\ 0 &= g(x, z, 0, p(x, z), w) \end{aligned} \tag{19}$$

Using that the second equation has a unique, isolated solution $z = \hat{g}(x, w)$ (Assumption 1), we can re-write (19) as follows:

$$\frac{dx}{dt} = f(x, \hat{g}(x, w), 0, u_s^*, w) = f_s(x, u_s^*, w) \tag{20}$$

According to Proposition 1, the state $x(t)$ of the closed-loop slow subsystem of Eq. (20) starting from $x(0) \in \Omega_\rho$ stays in Ω_ρ (i.e., $x(t) \in \Omega_\rho\ \forall t \geq 0$) and satisfies the bound of Eq. (16).

We now turn to the fast subsystem. Using $\tau = (t/\epsilon)$ and $y = z - \hat{g}(x, w)$, the closed-loop system of Eq. (18) can be written as:

$$\begin{aligned} \frac{dx}{d\tau} &= \epsilon f(x, y + \hat{g}(x, w), \epsilon, u_s(x), w) \\ \frac{dy}{d\tau} &= g(x, y + \hat{g}(x, w), \epsilon, p(x, y), w) - \epsilon\frac{\partial\hat{g}}{\partial w}\dot{w} \\ &\quad - \epsilon\frac{\partial\hat{g}}{\partial x} f(x, y + \hat{g}(x, w), u_s(x), w) \end{aligned} \tag{21}$$

Setting $\epsilon = 0$, the closed-loop fast subsystem is obtained:

$$\frac{dy}{d\tau} = g(x, y + \hat{g}(x, w), 0, p(x, y), w) \tag{22}$$

According to Assumption 2, the origin of the system of Eq. (22) is globally asymptotically stable, uniformly in $x \in R^n$ and $w \in R^l$ in the sense that there exists a class *KL* function β_y such that for any $y(0) \in R^m$, the bound of Eq. (9) holds for $t \geq 0$. Therefore, the closed-loop system of Eq. (18) satisfies the assumptions 1, 2 and 3 of Theorem 1 in [18]. Thus, there exist functions β_x and β_y of class *KL*, positive real numbers (δ, d) (note that the existence of δ such that $|x(0)| \leq \delta$ implies that $x(0) \in \Omega_\rho$ follows from the smoothness of $V(x)$), and $\epsilon^* > 0$ such that if $\max\{|x(0)|, |y(0)|, ||w||, ||\dot{w}||\} \leq \delta$ and $\epsilon \in (0, \epsilon^*]$, then, the bounds of Eq. (17) hold for all $t \geq 0$. □

Remark 1. We note that the class of nonlinear systems of Eq. (1) can be generalized to include: (a) u_s in the g vector field (i.e., the manipulated inputs that are used to control the slow subsystem affect directly the fast dynamics) and (b) u_f in the f vector field (i.e., the manipulated inputs that are used to control the fast subsystem affect directly the slow dynamics). Such a generalization would simply require that u_s, which is computed by the MPC and is piecewise continuous in time, is passed through an appropriate filter to become absolutely continuous (see also Theorem 1 and Remark 1 in [18]); this generalization is not pursued here in order to avoid complicating further the notation. We also note that instead of using the LMPC of Eq. (13) other MPC schemes including distributed MPC schemes can be used to control the slow subsystem and they will inherit the stability properties of Theorem 1 as long as these MPC schemes satisfy the conditions of Proposition 1.

4. Application to a nonlinear large-scale process network

4.1. Process description and control system design

The process considered in this study is a reactor-distillation process network, shown in Fig. 2 (see also [2]). It consists of a continuously stirred tank reactor (CSTR), a distillation tower including a reboiler and a condenser, and a recycle loop. A set of elementary exothermic reactions in series takes place in the reactor of the form $A \xrightarrow{k_1} B \xrightarrow{k_2} C$, in which A is the reactant, B is the desired product and C is the by-product. The reactor is fed with a fresh feed of pure species A at flowrate F_0. The outlet of the reactor is fed into the distillation tower, where most of the reactant A is separated overhead and recycled back to the CSTR, and most of the product and the by-product leave the system through stream B_t. There are three heat/coolant inputs, labeled as Q_1, Q_2, and Q_3, that are assigned to the CSTR, the condenser, and the reboiler, respectively. The flow rates of streams F, D and B_t are regulated by three valves, labeled as $V1$, $V2$, and $V3$, respectively. The dynamic equations describing the behavior of the process are obtained through material and energy balances under standard modeling assumptions. Specifically, the dynamic model of the CSTR is as follows:

$$\dot{M}_R = F_0 + D - F \tag{23a}$$

$$\dot{x}_{A,R} = \frac{F_0(1 - x_{A,R}) + D(x_{A,0} - x_{A,R})}{M_R} - k_1 e^{-E_1/RT} x_{A,R} \tag{23b}$$

$$\dot{x}_{B,R} = \frac{-F_0 x_{B,R} + D(x_{B,0} - x_{B,R})}{M_R} + k_1 e^{-E_1/RT} x_{A,R} - k_2 e^{-E_2/RT} x_{B,R} \tag{23c}$$

$$\dot{H}_{L,R} = \frac{F_0(H_{L,F_0} - H_{L,R}) + D(H_{L,0} - H_{L,R})}{M_R} + \frac{Q_1}{M_R} - k_1 e^{-E_1/RT} x_{A,R} \Delta H_{r1} - k_2 e^{-E_2/RT} x_{B,R} \Delta H_{r2} \tag{23d}$$

The dynamic model of the condenser is as follows:

$$\dot{M}_0 = \bar{V} - R - D \tag{24a}$$

$$\dot{x}_{i,0} = \frac{\bar{V}}{M_0}(y_{i,1} - x_{i,0}) \tag{24b}$$

$$\dot{H}_{L,0} = \frac{\bar{V}}{M_0}(H_{V,1} - H_{L,0}) + \frac{Q_2}{M_0} \tag{24c}$$

where $i = A, B, C$. The dynamic model of the distillation column is as follows:

$$\dot{x}_{i,j} = \frac{1}{M_j}[\bar{V}(y_{i,j+1} - y_{i,j}) + R(x_{i,j-1} - x_{i,j})], \quad 1 \leq j < f \tag{25a}$$

$$\dot{H}_{L,j} = \frac{\bar{V}}{M_j}(H_{V,j+1} - H_{V,j}) + \frac{R}{M_j}(H_{L,j-1} - H_{L,j}), \quad 1 \leq j < f \tag{25b}$$

$$\dot{x}_{i,f} = \frac{1}{M_f}[\bar{V}(y_{i,f+1} - y_{i,f}) + R(x_{i,f-1} - x_{i,f}) + F(x_{i,R} - x_{i,f})], \quad j = f \tag{25c}$$

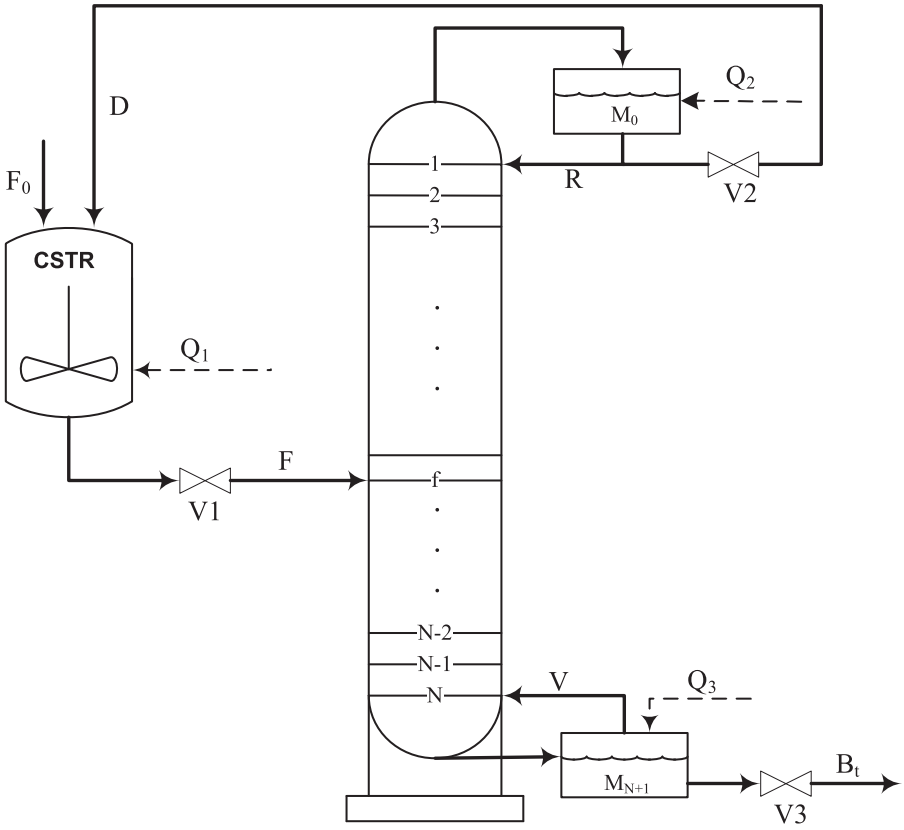

Fig. 2. Chemical process network schematic.

$$\dot{H}_{L,f} = \frac{\bar{V}}{M_f}(H_{V,f+1} - H_{V,f}) + \frac{R}{M_f}(H_{L,f-1} - H_{L,f}) + \frac{F}{M_f}(H_{L,R} - H_{L,f}), \quad j = f \tag{25d}$$

$$\dot{x}_{i,j} = \frac{1}{M_j}[\bar{V}(y_{i,j+1} - y_{i,j}) + (R+F)(x_{i,j-1} - x_{i,j})], \quad f < j \le N \tag{25e}$$

$$\dot{H}_{L,j} = \frac{\bar{V}}{M_j}(H_{V,j+1} - H_{V,j}) + \frac{R+F}{M_j}(H_{L,j-1} - H_{L,j}), \quad f < j \le N \tag{25f}$$

where $i = A, B, C$ and N is the number of column stages. Finally, the dynamic model of the reboiler is as follows:

$$\dot{M}_{N+1} = R + F - \bar{V} - B_t \tag{26a}$$

$$\dot{x}_{i,N+1} = \frac{1}{M_{N+1}}[(R+F)(x_{i,N} - x_{i,N+1}) - \bar{V}(y_{i,N+1} - x_{i,N+1})] \tag{26b}$$

$$\dot{H}_{L,N+1} = \frac{R+F}{M_{N+1}}(H_{L,N} - H_{L,N+1}) - \frac{\bar{V}}{M_{N+1}}(H_{V,N+1} - H_{L,N+1}) + \frac{Q_3}{M_{N+1}} \tag{26c}$$

where $i = A, B, C$. The definitions of the process parameters and their nominal values are given in Tables 1 and 2, respectively.

The model of the CSTR assumes perfect mixing and spatially uniform heat conduction. Both reactions in the reactor are first-order elementary reactions. The composition of species C can be computed by the following relationship, $x_{A,R} + x_{B,R} + x_{C,R} = 1$. For the derivation of the dynamic model of the multicomponent distillation, we apply stage-by-stage methods and batch rectification. To apply this approach, we assume vapor–liquid equilibrium in each stage, perfect mixing of liquid and vapor in each stage, negligible vapor holdup, constant-molar-liquid holdup, M_j, on each stage, and adiabatic process for the entire distillation process. In this work, the thermodynamic properties of the mixtures are obtained by assuming ideal behavior in both liquid phase and vapor phase. Specifically, the enthalpy of each species in vapor state is described by the following expression:

$$h_{V,i} = h^o_{V,i} + C_{P_V,i}(T - T_0)$$

Table 1
Process variables.

$F_0, D, F, R, \bar{V}, B$	Effluent flow rates
$\tilde{F}_0, \tilde{D}, \tilde{F}, \tilde{R}, \tilde{V}, \tilde{B}$	Steady-state values of effluent flow rates
$x_{i,R}$	Species composition in the CSTR
$x_{i,j}$	Species composition in the distillation tower
M_R, M_0, M_{M+1}	Liquid hold-up in each vessel
$C_{P_V,i}$	Heat capacity of each species at vapor phase
α_i	Relative volatilities of each species
$\Delta H_{r1}, \Delta H_{r2}$	Heat of reactions 1 and 2
$H_{V,R}$	Enthalpy of mixture in the CSTR
$H_{V,j}$	Enthalpy of gas mixture
$H_{L,j}$	Enthalpy of liquid mixture
H_{L,F_0}	Enthalpy of feed input
k_1, k_2	Reaction coefficient
E_1, E_2	Activation energy
Q_1, Q_2, Q_3	External heat/coolant inputs to each vessel

Table 2
Parameter values.

ΔH_{r1}	2500 [J/mol]	ΔH_{r2}	5500 [J/mol]
E_1	9500 [J/mol]	E_2	12,000 [J/mol]
k_1	2.4 [1/s]	k_2	4.0 [1/s]
$F_0, \tilde{F}_0$	100 [mol/s]	H_{L,F_0}	61.06 [J/mol]

Table 3
Process parameters.

	A	B	C
$C_{p_V,i}$ [J/mol K]	1.86	2.01	2.00
ΔH_i^{Vap} [J/mol]	83.333	86.111	85.556
$h^o_{V,i}$ [J/mol]	283.889	369.844	394.444
α_i	5.5	1.2	1.0

where T_0 is the reference temperature and its value is 373.15 K, $h^o_{V,i}$ is the enthalpy of a species at the reference temperature and $C_{P_V,i}$ is the heat capacity of a species and is assumed to be a constant. The derivation of the enthalpy of a vapor mixture and the enthalpy of a liquid mixture, based on above assumptions, is given by:

$$H_V = \sum_i^{A,B,C} y_i h^0_{V,i} + (T - T_0) \sum_i^{A,B,C} y_i C_{p_V,i}$$
$$H_L = \sum_i^{A,B,C} x_i (h^0_{V,i} - \Delta H_i^{Vap}) + (T - T_0) \sum_i^{A,B,C} x_i C_{p_V,i} \quad (27)$$

If the enthalpy of a liquid mixture is known, we can obtain the temperature using the following expression:

$$T = \frac{H_L - \sum_i^{A,B,C} x_i (h^0_{V,i} - \Delta H_i^{Vap})}{\sum_i^{A,B,C} x_i C_{p_V,i}} + T_0$$

Furthermore, the enthalpy of the vapor mixture can be obtained by substituting the computed temperature value back into Eq. (27). For ideal liquid–vapor mixture, Raoult's law determines the relationship between the vapor phase molar composition and the liquid phase molar composition of each species. In this model, we assume that the vapor pressure of each species, or the relative volatility of each species, is a constant. Hence, the following equation, based on Raoult's law, can be used to compute the vapor phase molar composition, once the liquid phase molar composition is known:

$$y_i = \frac{\alpha_i x_i}{\sum_k^{A,B,C} \alpha_k x_k}$$

For the other thermodynamic parameters, one can refer to Table 3 for their nominal values. The distillation tower has a total of 15 trays, and the reactor outlet is fed into tray 12. The entire process network has a total of 57 states which consist of the compositions of A, B, and C in the reactors, column stages, reboiler and condenser, as well as the enthalpy in each of the vessels. The desired (final) operating point of the process, corresponding to the seven steady-state manipulated input values, $\tilde{F}$, $\tilde{V}$, $\tilde{B}$, $\tilde{R}$, $\tilde{D}$, $\tilde{Q}_1$, $\tilde{Q}_2$, and $\tilde{Q}_3$ (Table 4), is given in Table 5.

The goal of the controller is to drive the system from the initial stable operating point to the desired operating point. The initial steady-state values for the manipulated inputs and the states of the CSTR, reboiler and condenser are given in Tables 6 and 7, respectively. Before proceeding with the control design, we note that via extensive simulation we have verified that the process exhibits two-time-scale behavior (see Fig. 12) owing to the use of large recycle, D, relative to the feed input, F_0, which motivates defining $\epsilon = \tilde{F}_o/\tilde{D} = 0.056$. However, several of the process states exhibit dynamic behavior in both fast and slow time scales, and thus, the explicit separation of the process model states into fast and slow ones in a way that it is consistent with the standard singularly perturbed model form of Eq. (1) is not a feasible task in this particular application. For this reason, instead of separating the states into fast and slow ones, we divide the manipulated inputs into the ones that regulate critical fast states and the ones that regulate the process state in the slow time-scale. Specifically, we define the following dimensionless manipulated inputs, $u_1 = F/\tilde{F}$, $u_2 = \bar{V}/\tilde{V}$, $u_3 = B_t/\tilde{B}_t$, $u_4 = D/\tilde{D}$, $u_5 = Q_1/\tilde{Q}_1$, $u_6 = Q_2/\tilde{Q}_2$ and $u_7 = Q_3/\tilde{Q}_3$. Through extensive simulations, we found that the manipulated inputs, u_1, u_2, u_3 and u_4 can be used to control the liquid hold-ups (fast dynamics), and u_5, u_6 and u_7 can be used to control the process state in the slow time-scale; see Remark 2 below for a detailed discussion and simulations on this issue.

With respect to control design, we propose to design a control system that utilizes proportional control to compute the inputs associated with the fast dynamics and MPC to compute the inputs associated with the slow dynamics. Specifically, four different proportional controllers are used to regulate each of the flow rates, F, D, $\bar{V}$, and B with respect to the final steady-state input values in Table 4 and the steady-state liquid holdups in Table 5:

$$u_1 = \frac{F}{\tilde{F}} = 1 - k_{c1}(\tilde{M}_R - M_R) \quad (28a)$$

Table 7
Initial steady state values of the states of CSTR, reboiler and condenser.

M_R	1300 [mol]	$x_{A,R}$	0.763
M_0	1125 [mol]	$x_{A,0}$	0.806
M_{N+1}	1425 [mol]	$x_{A,N+1}$	0.00159
$x_{B,R}$	0.210	$H_{L,R}$	1.966×10^2 [J/mol]
$x_{B,0}$	0.176	$H_{L,0}$	2.047×10^2 [J/mol]
$x_{B,N+1}$	0.800	$H_{L,N+1}$	3.880×10^2 [J/mol]

Table 4
Final steady-state manipulated input values.

$\tilde{Q}_1$	2.85×10^5 [J/s]	$\tilde{Q}_2$	-1.93×10^5 [J/s]	$\tilde{Q}_3$	2.31×10^5 [J/s]	$\tilde{F}$	1880 [mol/s]
$\tilde{V}$	2070 [mol/s]	$\tilde{B}_t$	100 [mol/s]	$\tilde{D}$	1780 [mol/s]	$\tilde{R}$	290 [mol/s]

Table 5
Final steady-state values of the states of CSTR, reboiler and condenser.

$\tilde{M}_R$	1100 [mol]	$\tilde{M}_0$	1050 [mol]	$\tilde{M}_{N+1}$	1200 [mol]
$\tilde{x}_{A,R}$	0.897	$\tilde{x}_{A,0}$	0.948	$\tilde{x}_{A,N+1}$	0.00666
$\tilde{x}_{B,R}$	0.0965	$\tilde{x}_{B,0}$	0.0505	$\tilde{x}_{B,N+1}$	0.916
$\tilde{H}_{L,R}$	1.849×10^2 [J/mol]	$\tilde{H}_{L,0}$	1.952×10^2 [J/mol]	$\tilde{H}_{L,N+1}$	3.826×10^2 [J/mol]

Table 6
Initial steady-state manipulated input values.

Q_1	3.58×10^5 [J/s]	Q_2	-2.00×10^5 [J/s]	Q_3	2.335×10^5 [J/s]	F	1880 [mol/s]
V	2070 [mol/s]	B_t	100 [mol/s]	D	1780 [mol/s]	R	290 [mol/s]

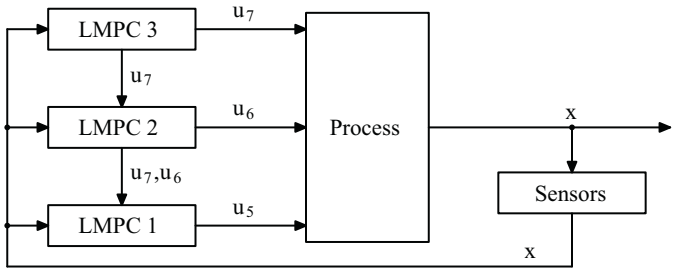

Fig. 3. Sequential DMPC architecture manipulating u_5, u_6 and u_7.

$$u_2 = \frac{\bar{V}}{\tilde{\bar{V}}} = 1 - k_{c2}(\tilde{M}_{N+1} - M_{N+1}) \tag{28b}$$

$$u_3 = \frac{B}{\tilde{B}} = 1 - k_{c3}(\tilde{M}_0 - M_0) \tag{28c}$$

$$u_4 = \frac{D}{\tilde{D}} = 1 - k_{c4}(\tilde{M}_0 - M_0) \tag{28d}$$

in which k_{c1}, k_{c2}, k_{c3} and k_{c4} are all equal to 0.0001. The controllers of Eq. (28) utilize feedback of the hold-ups that can be sampled fast and can stabilize the liquid hold-up levels of the CSTR, the reboiler and the condenser. Note that the effluent flow rate of the vapor mixture $\bar{V}$ is also regulated by a pressure valve. When the pressure inside the reboiler goes down, the rate of liquid evaporation rises and therefore, the flow rate $\bar{V}$ goes up. In this example, we do not consider the pressure effect in the process model and assume that $\bar{V}$ is controllable and is directly related to the liquid holdup of the reboiler.

The control of the slow dynamics involves the application of MPC. Three MPC strategies are applied and compared in this study. Specifically, a centralized LMPC which calculates all the inputs in one optimization problem, a sequential distributed MPC (DMPC) in which the control inputs are calculated by distributed optimization problems in sequence, and an iterative DMPC in which the control inputs are evaluated by parallel distributed optimization problems solved in an iterative fashion. For more discussion on the sequential and iterative DMPC, refer to [19]. We define the term *evaluation number* to indicate the number of evaluations for the optimization problem solved in each controller at each sampling time. For instance, an evaluation number of one implies that there is no information sharing between the controllers, and each one of them returns the manipulated input values after the end of one evaluation.

Three distributed LMPCs are designed for both DMPC control strategies. In both strategies, LMPC 1 determines the input Q_1, LMPC 2 determines the input Q_2, and LMPC 3 determines the input Q_3. Schematics of the sequential and iterative DMPC architectures for this process are shown in Figs. 3 and 4, respectively. In order to formulate each of the optimization problems of the DMPCs (see [19]), the following feedback laws are used as the reference control laws in the design of the three LMPCs:

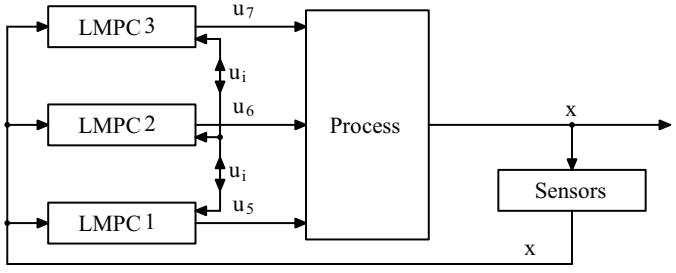

Fig. 4. Iterative DMPC architecture manipulating u_5, u_6 and u_7.

$$u_5 = \frac{Q_1}{\tilde{Q}_1} = 1 + k_{c5}(\tilde{T}_1 - T_1) \tag{29a}$$

$$u_6 = \frac{Q_2}{\tilde{Q}_2} = 1 + k_{c6}(\tilde{T}_2 - T_2) \tag{29b}$$

$$u_7 = \frac{Q_3}{\tilde{Q}_3} = 1 + k_{c7}(\tilde{T}_2 - T_3) \tag{29c}$$

where $k_{c5} = 0.008$, $k_{c6} = 0.0002$, $k_{c7} = 0.0002$, $\tilde{T}_1 = 360.25$, $\tilde{T}_2 = 367.97$ and $\tilde{T}_3 = 421.72$. In the design of the LMPCs, a quadratic Lyapunov function $V(x) = x^T P x$ where P is an identity matrix used to put even weights on the different states. Through extensive simulations, we found this Lyapunov function choice to be a good one in terms of control performance and ease of controller implementation. In the simulations, the inputs associated with the slow dynamics are subject to the following constraints:

$$0.9 \le u_5 \le 1.3, \quad 0.9 \le u_6 \le 1.2, \quad 0.9 \le u_7 \le 1.2.$$

4.2. Simulation results

The simulations were performed in Microsoft Visual Studio by a Core2 Quad Q6600 computer. The total process evaluation time for each run is 3000 s. Four different cases are studied here. The first one applies the centralized LMPC scheme. The second case is for the sequential DMPC approach. In the third and fourth case study, the iterative DMPC scheme with one evaluation and two evaluations are used. Two different prediction horizons are used for each of the MPC methods, $N = 1$ and $N = 2$. Only the first input value from the output of the optimization problems is implemented following a receding horizon scheme. The sampling time of the optimization problems is $\Delta = 30$ s, and as a result, the total number of sampling times along one simulation is 100. By assumption, all state measurements are available to the MPC controllers at each sampling time and are available continuously to the proportional controllers. The numerical method that is used to integrate the process is explicit Euler with a fixed time step of 0.1 s and the LMPC optimization problems are solved using the open source interior point optimizer Ipopt [20].

The cost function used in each MPC scheme is as follows:

$$J = \int_{t_k}^{t_{k+N}} \left[x^T(t) Q_c x(t) + U_2^T(t) R_{ci} U_2(t) \right] dt$$

where t_k is time when the controller is evaluated and $U_2^T = [u_5 - 1\ u_6 - 1\ u_7 - 1]$. The weighting matrix Q_c is a diagonal matrix with its diagonal element $Q_{c,i} = 1/x_{set,i}$, where $x_{set,i}$ is the steady state value of the corresponding state variable. The weighting matrix R_{c2} is also a diagonal matrix with $R_{c2} = 10,000 I_{3\times 3}$ where $I_{3\times 3}$ is the identity matrix of dimension 3×3.

Fig. 5 shows the trajectories of the Lyapunov function $V(x)$ under the different control schemes. Based on these trajectories, it can be seen that all MPC strategies stabilize the closed-loop system and give very close results in terms of trajectories of $V(x)$. The corresponding trajectories of the inputs Q_1, Q_2 and Q_3 (i.e., u_5, u_6 and u_7) are shown in Figs. 6–8.

Next, we investigate the instantaneous closed-loop performance at each sampling time measured by $x^T(t_k) Q_c x(t_k) + \sum_{i=1}^{2} U_i^T(t_k) R_{ci} U_i(t_k)$, $k = 0, 1, \ldots$ under the centralized LMPC and the two DMPC schemes where $U_1^T = [u_1 - 1\ u_2 - 1\ u_3 - 1\ u_4 - 1]$ and $R_{c1} = 10,000 I_{4\times 4}$ where $I_{4\times 4}$ is the identity matrix of dimension 4×4. The results are shown in Fig. 9. We note that in this cost we also include the control inputs used for the fast dynamics in order to have a comprehensive comparison. From Fig. 9,

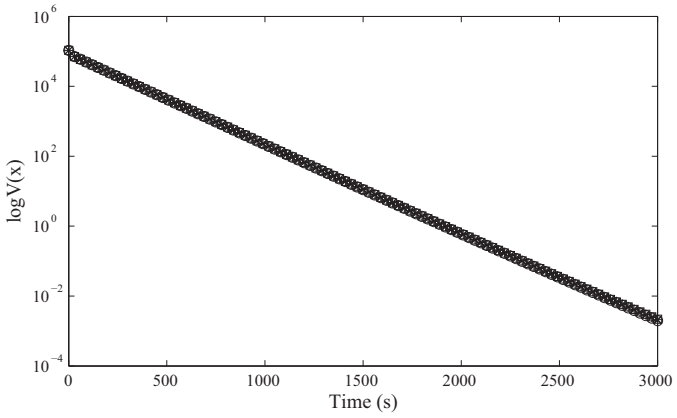

Fig. 5. Trajectories of $V(x)$ under the centralized LMPC (○), the sequential DMPC (∗), and the iterative DMPC with one evaluation (□) and with two evaluations (×).

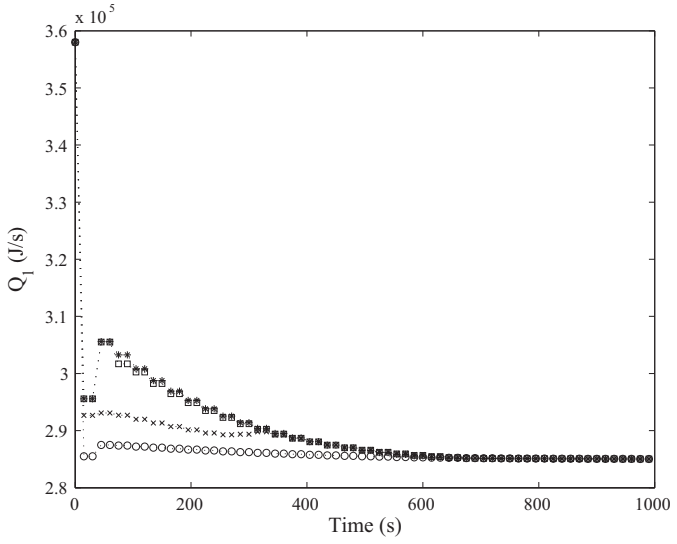

Fig. 6. Trajectories of the input Q_1 (i.e., u_5) under the centralized LMPC (○), the sequential DMPC (∗), and the iterative DMPC with one evaluation (□) and with two evaluations (×).

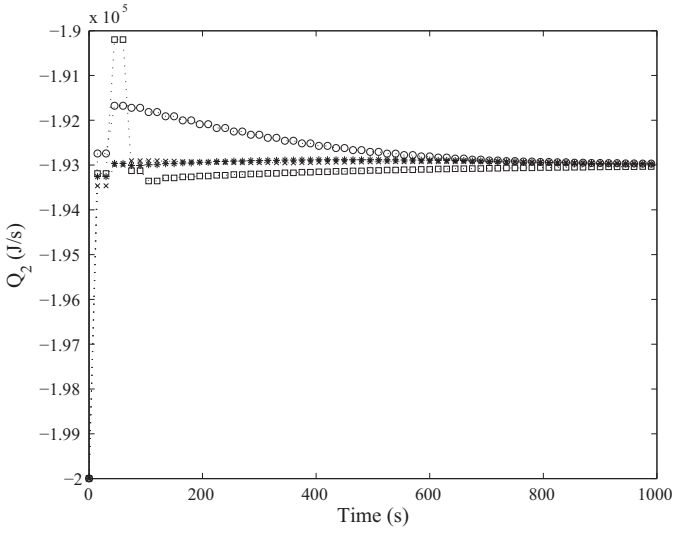

Fig. 7. Trajectories of the input Q_2 (i.e., u_6) under the centralized LMPC (○), the sequential DMPC (∗), and the iterative DMPC with one evaluation (□) and with two evaluations (×).

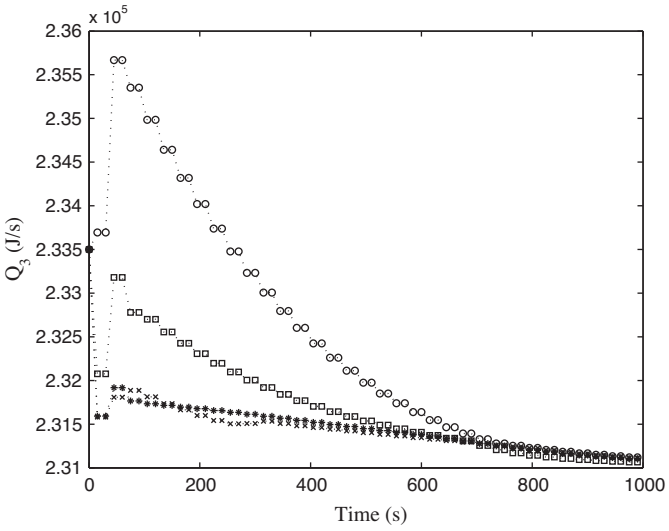

Fig. 8. Trajectories of the input Q_3 (i.e., u_7) under the centralized LMPC (○), the sequential DMPC (∗), and the iterative DMPC with one evaluation (□) and with two evaluations (×).

we see that as the simulation time approaches 1000 s, the instantaneous closed-loop performance given by the different control schemes is nearly the same. This is because under the different control schemes, the closed-loop system state is driven to the same desired steady-state. From Fig. 9 (especially from the first half of the simulation: $0 < t < 500$ s), we can also see that the centralized control scheme gives the best performance and as the iteration number increases, the performance given by the iterative DMPC converges to the one given by the centralized control scheme. This property of the iterative DMPC is not guaranteed for general nonlinear systems but it is found to hold for this specific simulation study.

In the last set of simulations, attention is given to the evaluation time of the three MPC schemes, as shown in Fig. 10 ($N = 1$) and in Fig. 11 ($N = 2$). Because of the different structures of the two DMPC architectures, it is important to note that the total evaluation time required for the sequential DMPC in one sampling time is the sum of the evaluation times of the three LMPCs; on the other hand, the total evaluation time required for the iterative DMPC with one evaluation in one sampling time is the maximum evaluation time among all the three LMPCs. Both figures clearly demonstrate that the iterative DMPC with one evaluation

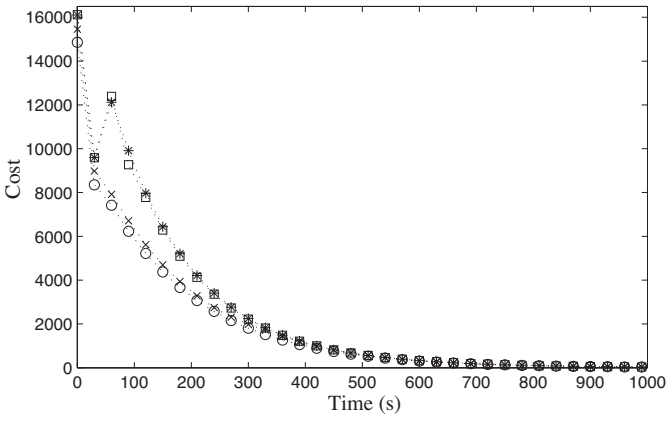

Fig. 9. The costs of the closed-loop system under the centralized LMPC (○), the sequential DMPC (∗), and the iterative DMPC with one evaluation (□) and with two evaluations (×).

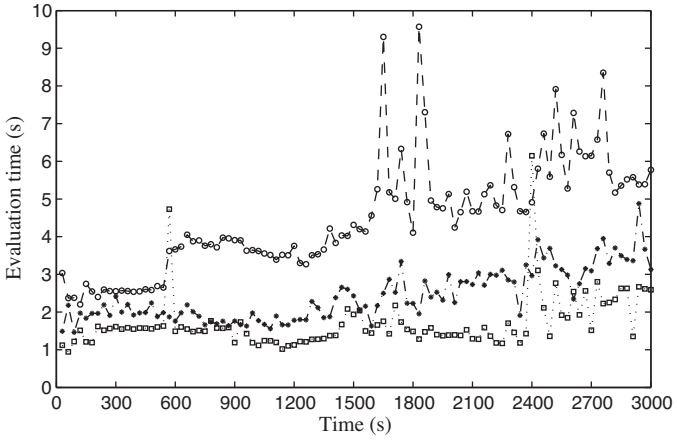

Fig. 10. The total evaluation time needed for each evaluation of each MPC method. Centralized LMPC (solid line with ∗), sequential DMPC (dashed line with ○), and iterative DMPC with one evaluation (dotted line with □). The prediction horizon $N = 1$.

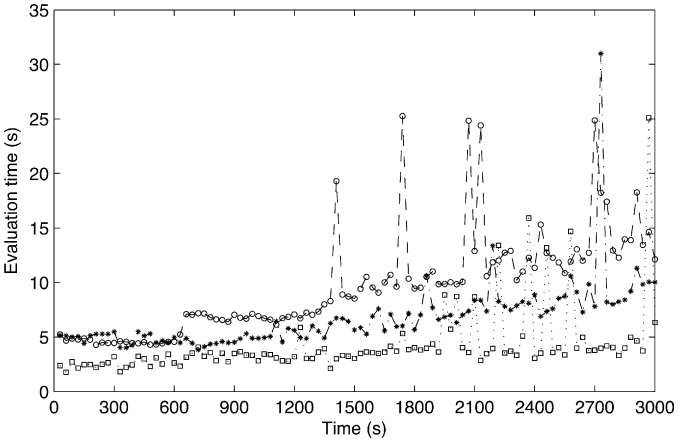

Fig. 11. The total evaluation time needed for each evaluation of each MPC method. Centralized LMPC (solid line with ∗), sequential DMPC (dashed line with ○), and iterative DMPC with one evaluation (dotted line with □). The prediction horizon $N = 2$.

has the smallest total evaluation time compared with the other MPC schemes, and the sequential DMPC requires more evaluation time than the centralized LMPC in this set of simulations. In Fig. 10, the average evaluation time of the iterative DMPC with one evaluation over the entire simulation is 1.70 s, which is about 70% of the average time needed for the centralized LMPC and 2.6 times faster than the average time needed for the sequential DMPC. Similarly, in Fig. 11, the average total evaluation time of the iterative DMPC with one evaluation along the simulation is 4.25 s, which is about 63% of the average time needed for the centralized LMPC and 2.3 times faster than the average time needed for the sequential DMPC.

Remark 2. To justify the use of u_1, u_2, u_3 and u_4 to control the liquid hold-ups that exhibit fast dynamic behavior, we carried out a set of simulations of the closed-loop system under the fast proportional controls used to manipulate u_1, u_2, u_3 and u_4 and the centralized MPC used to manipulate u_5, u_6 and u_7. Fig. 12 shows the evolution of a measure of the liquid hold-ups ($\rho_f(t)$) which exhibit fast dynamics initially (fast time-scale) and the evolution of a measure of the compositions ($\rho_s(t)$) which exhibit dynamics in a slow time-scale, thereby confirming our choice to use fast acting feedback to regulate the liquid hold-ups. In Fig. 12, the measures $\rho_s(t)$ and $\rho_f(t)$ are defined as follows:

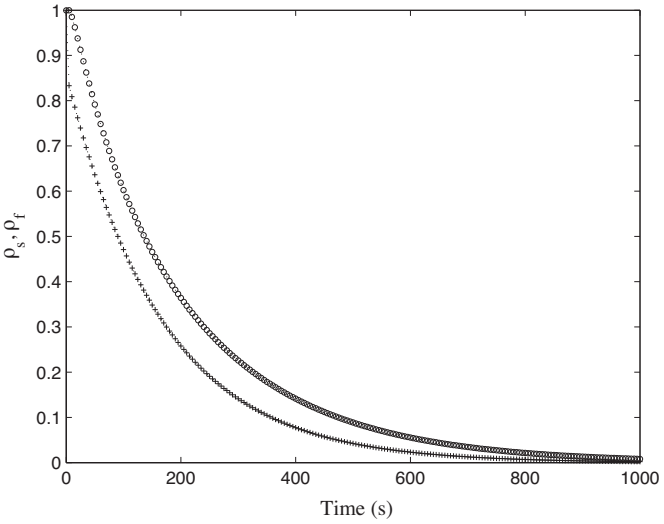

Fig. 12. Evolution of a measure of the liquid hold-ups ($\rho_f(t)$; + symbol) and evolution of a measure of the compositions ($\rho_s(t)$; o symbol).

$$\rho_s(t) = \frac{\sum_{i}^{A,B,C}\sum_{j}^{15}(x_{i,j} - \tilde{x}_{i,j})^2 + \sum_{i}^{A,B,C}(x_{i,R} - \tilde{x}_{i,R})^2}{\max((x_{i,j} - \tilde{x}_{i,j})^2, (x_{i,R} - \tilde{x}_{i,R})^2)} \tag{30a}$$

$$\rho_f(t) = \frac{(M_o - \tilde{M}_o)^2 + (M_{N+1} - \tilde{M}_{N+1})^2 + (M_R - \tilde{M}_R)^2}{\max((M_o - \tilde{M}_o)^2, (M_{N+1} - \tilde{M}_{N+1})^2, (M_R - \tilde{M}_R)^2)} \tag{30b}$$

5. Conclusions

This work focused on model predictive control of a class of nonlinear singularly perturbed systems. The motivation for this work is provided by broad classes of large-scale process networks that involve coupled variables that evolve in disparate (fast and slow) time scales. For such process networks, direct application of model predictive control to compute the control actions for all manipulated inputs leads to very high-order optimization problems that may not be solvable in real-time. Instead, we proposed a control system using multirate sampling (i.e., fast sampling of easy-to-measure fast-evolving variables and slow sampling of slow-evolving variables) and consisting of an explicit feedback controller that stabilizes the fast dynamics and a model predictive controller that stabilizes the slow dynamics and enforces desired performance objectives in the slow subsystem. In this way, the model predictive controller solves an optimization problem with a substantially smaller number of decision variables, and thus, it requires less computational time. Sufficient conditions under which the closed-loop system stability, accounting for multirate sampling and sample-and-hold implementation of the predictive controller, is guaranteed were provided. The applicability and effectiveness of the proposed control system was illustrated via a large-scale nonlinear reactor-separator process network which exhibits two-time-scale behavior and the computational effectiveness of distributed predictive control implementation was demonstrated.

References

[1] P.D. Christofides, P. Daoutidis, Feedback control of two-time-scale nonlinear systems, International Journal of Control 63 (1996) 965–994.

[2] A. Kumar, P. Daoutidis, Nonlinear dynamics and control of process systems with recycle, Journal of Process Control 12 (2002) 475–484.
[3] P. Kokotovic, H.K. Khalil, J. O'Reilly, Singular Perturbation Methods in Control: Analysis and Design, Academic Press, London, 1986.
[4] P.D. Christofides, A.R. Teel, P. Daoutidis, Robust semi-global output tracking for nonlinear singularly perturbed systems, International Journal of Control 65 (1996) 639–666.
[5] C.E. García, D.M. Prett, M. Morari, Model predictive control: theory and practice—a survey, Automatica 25 (1989) 335–348.
[6] D.Q. Mayne, J.B. Rawlings, C.V. Rao, P.O.M. Scokaert, Constrained model predictive control: stability and optimality, Automatica 36 (2000) 789–814.
[7] P. Mhaskar, N.H. El-Farra, P.D. Christofides, Stabilization of nonlinear systems with state and control constraints using Lyapunov-based predictive control, Systems and Control Letters 55 (2006) 650–659.
[8] J.B. Rawlings, B.T. Stewart, Coordinating multiple optimization-based controllers: new opportunities and challenges, Journal of Process Control 18 (2008) 839–845.
[9] R. Scattolini, Architectures for distributed and hierarchical model predictive control—a review, Journal of Process Control 19 (2009) 723–731.
[10] P.D. Christofides, J. Liu, D. Muñoz de la Peña, Networked and Distributed Predictive Control: Methods and Applications to Nonlinear Process Networks, Advances in Industrial Control Series, Springer-Verlag, London, 2011.
[11] M. Wogrin, L. Glielmo, An MPC scheme with guaranteed stability for linear singularly perturbed systems, in: Proceedings of 49th IEEE Conference on Decision and Control, Atlanta, GA, 2010, pp. 5289–5295.
[12] M.A. Brdys, M. Grochowski, T. Gminski, K. Konarczak, M. Drewa, Hierarchical predictive control of integrated wastewater treatment systems, Control Engineering Practice 16 (2008) 751–767.
[13] E.J. Van Henten, J. Bontsema, Time-scale decomposition of an optimal control problem in greenhouse climate management, Control Engineering Practice 17 (2009) 88–96.
[14] J.L. Massera, Contributions to stability theory, Annals of Mathematics 64 (1956) 182–206.
[15] Y. Lin, E.D. Sontag, Y. Wang, A smooth converse Lyapunov theorem for robust stability, SIAM Journal on Control and Optimization 34 (1996) 124–160.
[16] P.D. Christofides, N.H. El-Farra, Control of Nonlinear and Hybrid Process Systems: Designs for Uncertainty, Constraints and Time-delays, Springer-Verlag, Berlin, Germany, 2005.
[17] D. Muñoz dela Peña, P.D. Christofides, Lyapunov-based model predictive control of nonlinear systems subject to data losses, IEEE Transactions on Automatic Control 53 (2008) 2076–2089.
[18] P.D. Christofides, A.R. Teel, Singular perturbations and input-to-state stability, IEEE Transactions on Automatic Control 41 (1996) 1645–1650.
[19] J. Liu, X. Chen, D. Muñoz de la Peña, P.D. Christofides, Sequential and iterative architectures for distributed model predictive control of nonlinear process systems, AIChE Journal 56 (2010) 2137–2149.
[20] A. Wächterand, L.T. Biegler, On the implementation of primal-dual interior point filter line search algorithm for large-scale nonlinear programming, Mathematical Programming 106 (2006) 25–57.